

SUPERSTRONG OPTICAL FIELDS

PACS numbers: 42.65.Jx; 42.65.Re; 78.67.Bf
DOI: 10.1070/QE2014v044n08ABEH015529

Threshold energies for filamentation and spectral characteristics of supercontinuum generation in THEOS-based nanocomposite organosilicon media

Yu.N. Kulchin, A.Yu. Mayor, D.Yu. Proschenko, A.A. Chekhlenok, I.V. Postnova, S.S. Golik, O.A. Bukin, Yu.A. Shchipunov

Abstract. **We have experimentally determined the threshold energy for filamentation in THEOS-based hybrid silicate nanocomposite materials containing polysaccharides and hyperbranched polyglycidols and the conversion efficiency from the 800-nm femtosecond Ti:sapphire laser output to a supercontinuum in the range 420–700 nm. The addition of sodium hyaluronate (polysaccharide) and low concentrations of Au nanoparticles or CdS quantum dots with an average diameter of 3–5 nm has been shown to considerably reduce the threshold energy for filamentation and improve the laser output to supercontinuum conversion efficiency.**

Keywords: *femtosecond laser, filamentation, supercontinuum, conical emission, gold nanoparticles, CdS quantum dots.*

1. Introduction

To improve the efficiency of modern nonlinear optical devices, use is currently made of materials based on niobates [1], orthosilicates doped with various rare-earth elements [2] and noncentrosymmetric crystals with multifunctional properties [3], which possess a fast and strong response to an external field owing to nonlinear optical interactions. Another promising research direction is the biomimetic modelling of the immobilisation of an organic material in a silicate matrix. One important advantage of this approach to creating optical materials is the low cost of synthesis (as distinct from specialised inorganic compounds). To create novel composite materials, wide use is made of various biopolymers, including proteins and the various types of polysaccharides applied in the food and drug industries [4].

A rather promising strategy for creating novel materials for nonlinear optics is the use of hybrid materials containing nanoparticles of various metals. In recent years, distinctive features of interaction between laser radiation and such media have been the subject of both basic and applied research [5]. Interaction between laser radiation and materials containing metallic nanoparticles (including noble metal nanoparticles) occurs predominantly at localised surface plasmon resonances [6–8], which ensure a considerable local increase in electromagnetic field intensity [9]. Metallic nanostructures find wide practical application, suggesting that such materials have great potential. In particular, they considerably increase the signal and improve the resolving power in Raman spectroscopy, which, in turn, allows one to detect single molecules [10]. Structured films containing localised metallic plasmons enable optical signal switching with nanosecond resolution [11, 12]. Another rather important feature of metallic nanoparticles is that they have high nonlinear susceptibilities. In particular, in the case of aqueous colloids containing silver nanoparticles, their nonlinear refractive index at nonresonant plasmon frequencies may exceed that of fused silica by more than six orders of magnitude [13]. The incorporation of nanoparticles into the structure of other materials would be expected to ensure a significant increase in nonlinearity coefficients. Metallic nanoparticles enable the synthesis of novel media possessing negative nonlinear refractive indices [14, 15], which is a necessary condition for the ability to produce superlenses. Another important aspect of the application of such structures is the possibility of low-threshold supercontinuum generation [16–18], accompanied by filamentation [19–21] in the medium.

There is considerable interest in materials containing quantum dots (QDs): conductor and semiconductor nanocrystals. QDs exist when the Bohr exciton radius is greater than each of the dimensions of the nanoparticles. This leads to spatial limitations on exciton motion, which, in turn, result in quantum confinement and the associated quantum effects, including surface plasmon resonance and luminescence [22–24]. QDs possess unique optical properties, in particular, a very narrow, symmetrical emission peak, with the possibility of varying their emission wavelength by merely changing the size of the nanocrystals, and a high quantum yield. Moreover, they have higher photo- and chemical stability than do organic dyes. Because of this, QDs attracted increased attention from the very beginning and are widely used in a great diversity of applications, including luminescent materials, biosensors, medical diagnostics, photocatalysis, solar power conversion and optoelectronics [25–30].

Yu.N. Kulchin, A.Yu. Mayor, A.A. Chekhlenok Institute for Automation and Control Processes, Far Eastern Branch, Russian Academy of Sciences, ul. Radio 5, 690041 Vladivostok, Russia; e-mail: kulchin@iacp.dvo.ru, mayor@iacp.dvo.ru;
D.Yu. Proschenko, S.S. Golik Institute for Automation and Control Processes, Far Eastern Branch, Russian Academy of Sciences, ul. Radio 5, 690041 Vladivostok, Russia; Far Eastern Federal University, ul. Sukhanova 8, 690091 Vladivostok, Russia; e-mail: golik_s@mail.ru;
I.V. Postnova Far Eastern Federal University, ul. Sukhanova 8, 690091 Vladivostok, Russia; Institute of Chemistry, Far Eastern Branch, Russian Academy of Sciences, prosp. Stoletiya Vladivostoka 159, 690022 Vladivostok, Russia; e-mail: ipost@chem.dvgu.ru;
O.A. Bukin Admiral G.I. Nevelskoi Maritime State University, Verkhneportovaya ul. 50a, 690059 Vladivostok, Russia;
Yu.A. Shchipunov Institute of Chemistry, Far Eastern Branch, Russian Academy of Sciences, prosp. Stoletiya Vladivostoka 159, 690022 Vladivostok, Russia; e-mail: YAS@ich.dvo.ru

Received 10 April 2014
Kvantovaya Elektronika **44** (8) 793–797 (2014)
Translated by O.M. Tsarev

In this paper, we report our findings on the key features of interaction between femtosecond laser radiation and new optically transparent, biomimetic organosilicon materials and analyse the effect of various additives on filamentation processes and supercontinuum (SC) conical emission.

2. Experimental procedure and samples

Filamentation processes were investigated using the femtosecond laser system at the shared experimental facilities centre 'Laser Techniques for Characterisation of Condensed Media and Biological Objects and Environmental Monitoring', Institute for Automation and Control Processes, Far Eastern Branch, Russian Academy of Sciences (Vladivostok). The laser system generated femtosecond pulses down to 40 fs in duration with up to 7 mJ of energy (when two amplification stages were used) at a repetition rate of up to 1 kHz.

To study filamentation thresholds, we used the configuration schematised in Fig. 1. A Lazer laser system (Fig. 1a), which comprised a Tsunami femtosecond oscillator and a Spectra Physics Spitfire 40F-1k-5W amplifier, generated ~45-fs pulses at a wavelength of 800 nm with a bandwidth $\Delta\lambda_{FWHM}$ = 35 nm and pulse energies of up to 2.5 mJ (one amplifier). The beam diameter was 7 mm. To rule out damage to the samples and optimise SC generation conditions in our experiments, the pulse energy was tuned by varying the pump current of the amplifier, and the pulse repetition rate was varied in the range 10 to 1000 Hz. The laser output parameters were checked at intervals: the pulse duration was measured with a Spectra Physics PulseScout autocorrelator, and the pulse energy was determined using a Spectra Physics Model 407A power meter. Radiation was directed to them by flip mirrors (not shown in Fig. 1a). The laser beam was focused by a lens (L1) with a focal length of 1 m. A sample (S) in which filament formation was observed (Fig. 1a) was situated 25 cm from the focus of the lens. The area of the laser beam spot on the input face of the sample was 2.4 mm^2. Behind the sample, the incident radiation was suppressed by a set of filters (F1) (SZS-23, SZS-25 and Newport 10SWF-700-B) with a transmission band from 420 to 700 nm. To study the structure of the filaments, we used a Newport LBP-HR profilometer (P) with a set of switchable neutral filters (F3). To image the filament pattern, another lens (L2) was placed two focal lengths from the filament formation region in the sample (S) and from the profilometer (P).

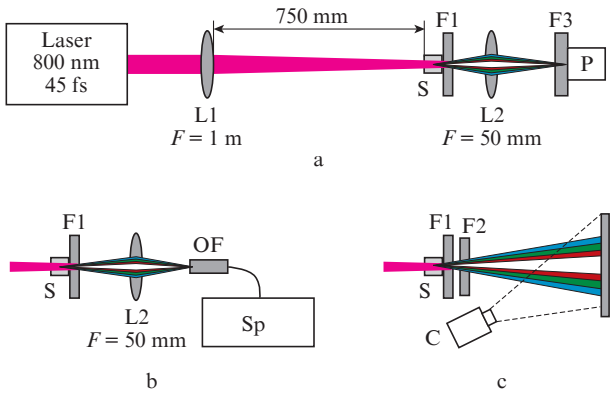

Figure 1. Schematic of the experimental setup:
(a) filament pattern imaging, (b) modified configuration for measuring the spectral characteristics of the SC, (c) modified configuration for SC conical emission imaging.

In studies of SC spectra, an optical fibre (OF) (Fig. 1b) with an opal diffuser (4-mm aperture) was used instead of the profilometer. The spectra were measured on an Ocean Optics Maya 2000Pro spectrometer (Sp). In SC power measurements in the visible range, a Gentec SOLO-2 power meter was used in place of the profilometer.

To study the spatial pattern of SC conical emission, we used a gridded screen (Fig. 1c), which was located 33 cm from the filamentation region. Images were recorded with a Canon 450D camera (C). Spectral ranges of interest were selected by interference filters (F2) (Fig 1c) with a transmission bandwidth of 10 nm FWHM (Thorlabs FKB-VIS-10 filter kit).

We studied monolithic nanocomposite materials prepared by a sol–gel process [31] using a completely water soluble precursor, tetrakis(2-hydroxyethyl) orthosilicate (THEOS) [32], with the addition of sodium hyaluronate (polysaccharide) or hyperbranched polyglycidols (HBPs) [33], and materials containing Au nanoparticles or CdS quantum dots. The key features of the synthesis of these materials were described in detail elsewhere [34]. Table 1 lists their compositions.

Table 1. Biomimetic organosilicon materials based on 50% THEOS + 50% H_2O.

Sample no.	Additive	wt % additive
1	No additive	
2	Na hyaluronate	0.125
3	Na hyaluronate	1
4	HBP	1
5	HBP + $HAuCl_4$	1 + 0.0008
6	CdS	0.1

3. Experimental results

In our experiments, we determined the filamentation thresholds in the samples studied. In sample 1 (THEOS with no additives), the threshold was 200 μJ. In THEOS containing sodium hyaluronate, a natural polysaccharide, the threshold energy for filament formation was observed to decrease with increasing polysaccharide concentration: from 130 μJ in sample 2, containing 0.125% sodium hyaluronate, to 60 μJ in sample 3, containing 1% sodium hyaluronate.

The incorporation of 1% HPB macromolecules to the THEOS matrix (sample 4) increased the threshold to 235 μJ. The addition of a trace amount of $HAuCl_4$ (0.0008%) to THEOS + 1% HBPs and subsequent formation of gold nanoparticles ~5 nm in size (sample 5) reduced the threshold by seven times relative to sample 1 (to 31 μJ). The incorporation of CdS quantum dots into THEOS (sample 6) reduced the threshold by a factor of 2.5 (to 80 μJ).

Figure 2 shows spatial intensity distributions in four samples near filamentation threshold (the distribution dimensions in the *xy* plane are 2×2 mm). According to these distributions, the filament diameter at half intensity ranges from 60 to 100 μm. The stable multiple filamentation thresholds were determined to be 245 (sample 1), 290 (sample 4), 77 (sample 5), 105 (sample 6), 200 (sample 2) and 76 μJ (sample 3).

For the samples with the lowest filamentation thresholds, we examined the effect of pulse energy on their SC spectra in the range 420–700 nm (Fig. 3). As the laser pulse energy increases near threshold, the SC spectrum gradually broadens to the anti-Stokes region. When the multiple filamentation threshold is reached, the intensity increases with increasing

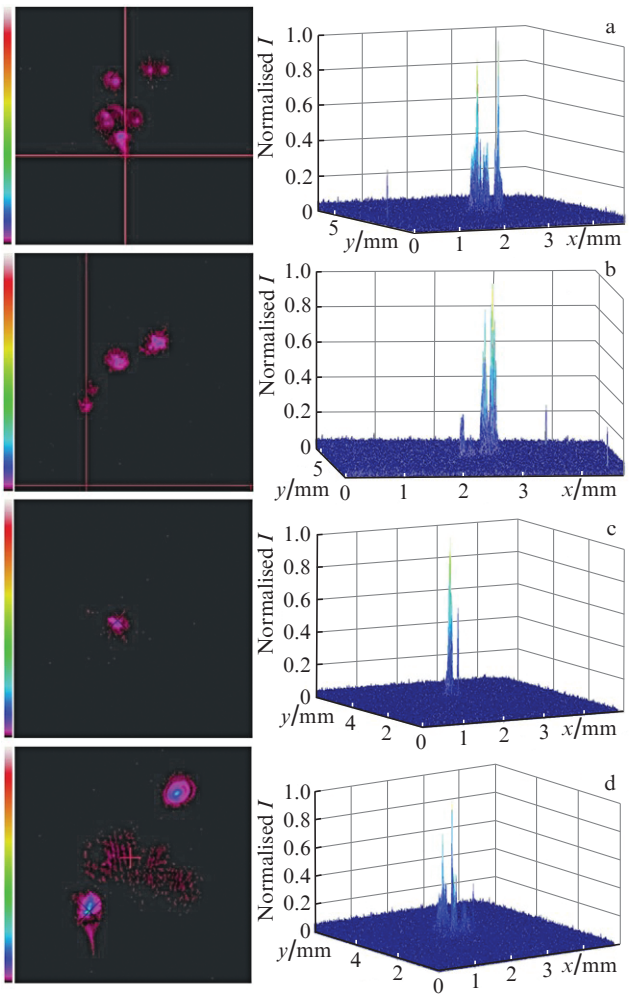

Figure 2. 2D and 3D intensity distributions in the case of threshold filamentation at a pulse duration of 45 fs and repetition rate of 100 Hz in samples (a) 1, (b) 3, (c) 6 and (d) 5.

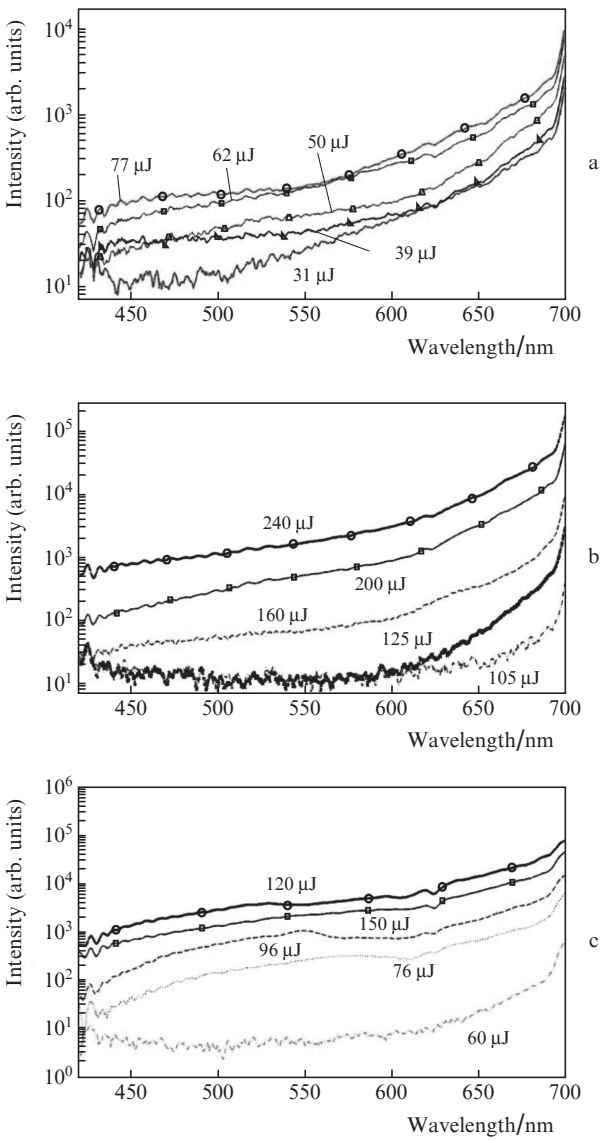

Figure 3. Effect of pulse energy on the SC spectra of samples (a) 5, (b) 6 and (c) 3 in the range 420–700 nm.

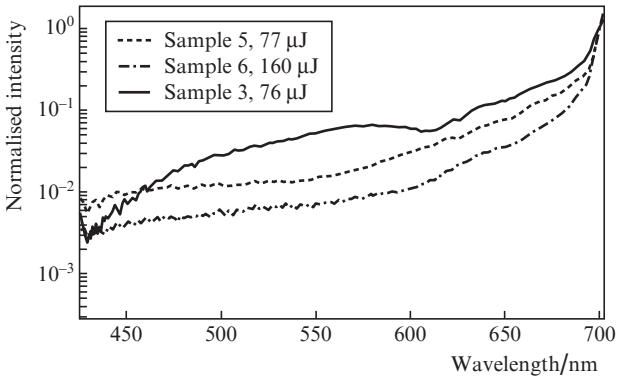

Figure 4. SC spectra of three samples in the range 420–700 nm under multiple filamentation conditions.

pulse energy throughout the spectrum. Figure 4 shows SC spectra normalised to the maximum intensity. It is seen from the spectral characteristics obtained that the highest intensity in the blue region of the SC spectrum is offered by the samples containing sodium hyaluronate and gold nanoparticles. The spectrum of the sample containing sodium hyaluronate has a characteristic local maximum in the range 500–550 nm.

Figure 5 shows the pulse-to-SC conversion efficiency in the range 420–700 nm for 45-fs laser pulses with a centre wavelength of 800 nm in the samples under consideration. The samples having lower filamentation thresholds offer higher conversion efficiency. According to the present results, some of the samples had threshold pulse energies above which incident laser radiation changed the filamentation properties of the material, without producing structural inhomogeneities or changing its absorption spectrum. The threshold for such modification was about 360 μJ in sample 5, containing gold nanoparticles, and 420 μJ in sample 6, containing CdS QDs. Note that the filamentation threshold in the modified samples increased to 180–200 μJ, and the laser pulse to SC conversion efficiency in them dropped markedly. Figure 6 illustrates the effect of such modification on conversion efficiency. Determination of the filamentation threshold in the modified samples a few hours and a day after the modification showed that the sample containing gold nanoparticles retained a high threshold, whereas the threshold in the sample containing CdS QDs decreased during the first few hours, without however reaching its original level.

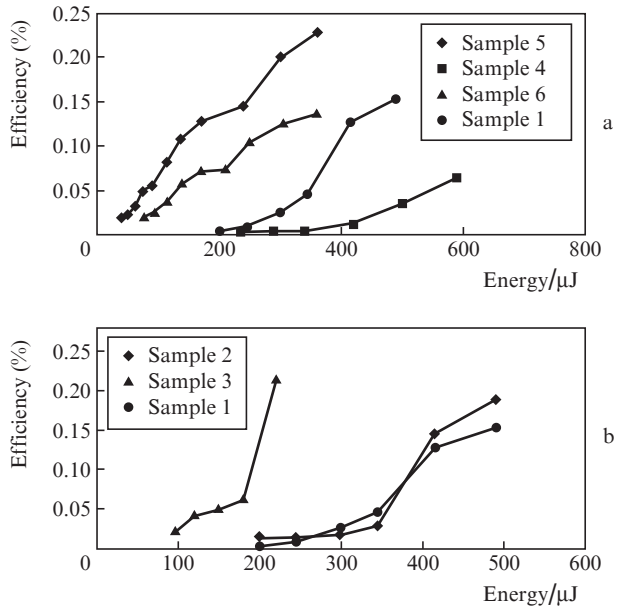

Figure 5. Laser pulse to SC conversion efficiency in the range 420–700 nm.

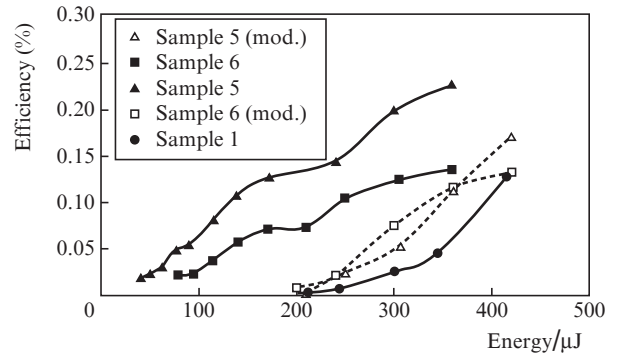

Figure 6. Conversion efficiency in some of the samples before (solid lines) and after (dashed lines) modification.

In studies of SC conical emission, we observed spatial separation into two regions: a central circle and a ring (Fig. 7). Such behaviour was reported previously for other materials, e.g. for water [35] (which accounted for about 50 wt% in the synthesis of our samples) and fused silica [36, 37]. With increasing pulse energy, a ring emerged in the SC conical emission, whereas only a central circle was observed at the threshold pulse energy for filamentation. When the pulse energy was raised to a level below the multiple filamentation threshold, a ring emerged in the 650-nm range. When the multiple filamentation threshold was reached, a ring emerged in the 600-nm range. At still higher pulse energies, a ring was present in the SC conical emission only in the 550-nm range, and there was no ring in the blue-green spectral region (450–500 nm) up to the highest permissible pulse energy. With increasing pulse energy, the position of the intensity maximum of the ring remained unchanged, but the divergence angle of the central circle in the SC conical emission increased until the circle merged with the ring, which correlates with previous results for fused silica [36, 37].

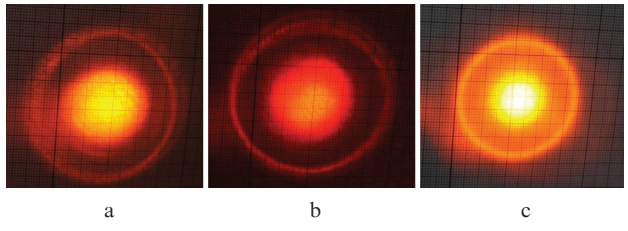

Figure 7. SC conical emission in the spectral range 600 ± 5 nm in (a) sample 5, (b) sample 4 and (c) distilled water.

The angle–frequency characteristics for the SC conical emission are linear in the regions of both the central circle and ring (Fig. 8). The characteristics for the rings differ little (within ±5%), except for the samples containing sodium hyaluronate, which had no ring in SC conical emission. Such behaviour of SC conical emission was also reported for other materials in the region of a negative or zero group velocity dispersion [35, 37].

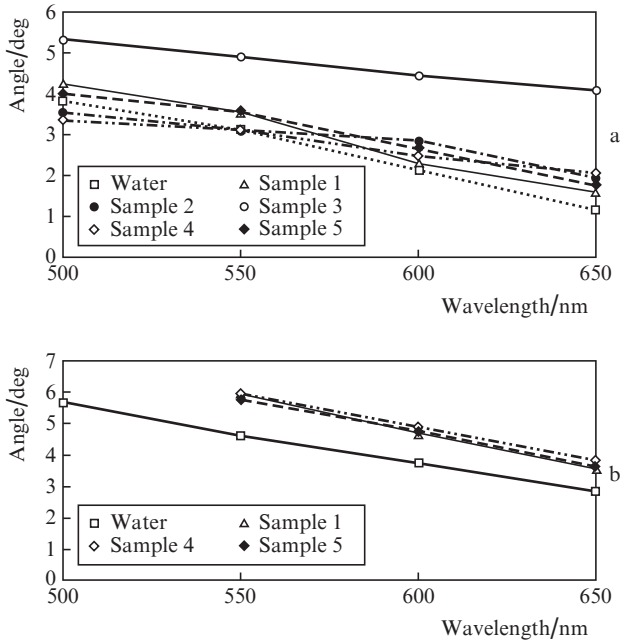

Figure 8. Angle–frequency characteristics of SC conical emission for the (a) central circle and (b) ring.

4. Conclusions

The incorporation of polysaccharides, Au + HBP nanoparticles and CdS QDs into THEOS considerably reduces the filamentation threshold of the material and improves the SC generation efficiency in the visible range. The addition of pure HBP raises the filamentation threshold but reduces the SC generation efficiency in the visible range. The materials containing Au + HBP nanoparticles and CdS QDs have threshold pulse energies above which incident laser radiation changes their filamentation properties, raising the filamentation threshold to the level of THEOS and reducing the SC generation efficiency. The changes in the materials containing Au + HBP nanoparticles are irreversible. The materials containing CdS QDs partly regain their properties over a period of several hours. We have obtained angle–frequency characteristics of

SC conical emission for a number of samples. The incorporation of sodium hyaluronate, a polysaccharide, has the strongest effect on the characteristics of SC conical emission in THEOS.

Acknowledgements. This research was supported by the Presidium of the Russian Academy of Sciences (Extreme Light Fields and Their Applications Programme).

References

1. Kaminskii A.A., Dong J., Eichler H.J., Hanuza J., Ueda K., Maczka M., Rhee H., Bettinelli M. *Laser Phys. Lett.*, **6**, 821 (2009).
2. Kaminskii A., Bagayev S.N., Ueda K., Dong J., Eichler H.J. *Laser Phys. Lett.*, **7**, 270 (2010).
3. Becker P., Bohaty L., Liebertz J., Kleebe H.-J., Muller M., Eichler H.J., Rhee H., Hanuza J., Kaminskii A.A. *Laser Phys. Lett*., **7**, 367 (2010).
4. Ruiz-Hitzky E., Darder M., Aranda P., in *Bio-inorganic Hybrid Nanomaterials* (Weinheim: Wiley-VCH, 2007) pp 1–40.
5. Pelton M., Aizpurua J., Bryant G. *Laser Photonics Rev*., **2**, 136 (2008).
6. Bohm D., Pines D. *Phys. Rev*., **82**, 625 (1951).
7. Govorov A., Richardson R. *Nano Today*, **2**, 1 (2007).
8. Kreibig U., Vollmer M. *Optical Properties of Metal Clusters* (Berlin: Springer, 1995).
9. Durach M., Rusina A., Stockman M.I., Nelson K. *Nano Lett*., **7**, 3145 (2007).
10. Nie S., Emory S.R. *Science*, **275**, 1102 (1997).
11. Sweatlock L.A., Maier S.A., Atwater H.A., Penninkhof J.J., Polman A. *Phys. Rev. B*, **71**, 235408 (2005).
12. Bozhevolnyi S., Volkov V., Devaux E., Ebbesen T. *Phys. Rev. Lett*., **95**, 046802 (2005).
13. Driben R., Husakou A., Herrmann J. *Opt. Lett.*, **34**, 14 (2009).
14. Murray W.A., Barnes W.L. *Adv. Mater.*, **19**, 3771 (2007).
15. Shalaev V.M. *Nat. Photonics*, **1**, 41 (2007).
16. Alfano R.R., Shapiro S.L. *Phys. Rev. Lett*., **24**, 584 (1970).
17. Driben R., Husakou A., Herrmann J. *Opt. Express*, **17**, 20 (2009).
18. Kulchin Yu.N., Golik S.S., Proschenko D.Yu., Chekhlenok A.A., Postnova I.V., Mayor A.Yu., Shchipunov Yu.A. *Kvantovaya Elektron*., **43**, 370 (2013) [*Quantum Electron*., **43**, 370 (2013)].
19. Kandidov V.P., Shlenov S.A., Kosareva O.G. *Kvantovaya Elektron*., **39**, 205 (2009) [*Quantum Electron*., **39**, 205 (2009)].
20. Kandidov V.P., Dormidonov A.E., Kosareva O.G., Akozbek N., Scalora M., Chin S.L. *Appl. Phys. B*, **87**, 29 (2007).
21. Couairon A., Mysyrowicz A. *Phys. Rep.*, **441**, 47 (2007).
22. Rogach A.L., Talapin D.V., Weller H. *Colloids and colloid assemblies* (Weinheim: Wiley-VCH, 2004).
23. Rempel' A.A. *Usp. Khim*., **76**, 474 (2007).
24. Schaefer H.-E. *Nanoscience. The Science of the Small in Physics, Engineering, Chemistry, Biology and Medicine* (Berlin: Springer, 2010).
25. Michalet X., Pinaud F.F., Bentolika L.A., et al. *Science*, **307**, 538 (2005).
26. Jiang W., Singhal A., Fischer H., et al., in *BioMEMS and Biomedical Nanotechnology, Vol. 3. Therapeutic Micro/ Nanotechnology* (New York: Springer, 2006) pp 137–156.
27. Lin C.-A.J., Li J.K., Sperling R.A., et al., in *Annual Review of Nanoresearch* (Singapore: World Scientific Publishing, 2006) pp 467–530.
28. Oleinikov V.A., Sukhanova A.V., Nabiev I.R. *Ross. Nanotekhnol.*, **2**, 160 (2007).
29. de Dios A.S., Diaz-Garcia M.E. *Anal. Chim. Acta*, **666**, 1 (2010).
30. Purcell-Milton F., Gun'ko Y.K. *J. Mater. Chem*., **22**, 16687 (2012).
31. Brinker C.J. *Sol–Gel Science: The Physics and Chemistry of Sol–Gel Processing* (San Diego, California: Academic Press, 1990) Vol. 3, p. 522.
32. Shchipunov Yu. A., in *Bio-inorganic Hybrid Nanomaterials* (Weinheim: Wiley, 2007).
33. Wilms D., Stiriba S.E., Frey H. *Acc. Chem. Res.*, **43**, 129 (2009).
34. Postnova I., Bezverbny A., Golik S., Kulchin Yu., Li H., Wang J., Kim I., Ha C-S., Shchipunov Yu. *Int. Nano Lett.*, **2**, 12 (2012).
35. Porras A.M., Dubietis A., Kucinskas E., Bragheri F., Degiorgio V., Couairon A., Faccio D., Trapani P.D. *Opt. Lett.*, **30**, 24 (2005).
36. Dormidonov A.E., Kandidov V.P., Kompanets V.O., Chekalin S.V. *Kvantovaya Elektron*., **39**, 653 (2009) [*Quantum Electron*., **39**, 653 (2009)].
37. Kandidov V.P., Smetanina E.O., Dormidonov A.E., Kompanets V.O., Chekalin S.V. *Zh. Eksp. Teor. Fiz*., **140**, 3 (2011).